ACS APPLIED MATERIALS & INTERFACES

Research Article

www.acsami.org

Tailored Nanoporous Coatings Fabricated on Conformable Polymer Substrates

David J. Poxson,*[,†] Frank W. Mont,[§] Jaehee Cho,[§] E. Fred Schubert,[§] and Richard W. Siegel[‡]

[†]Rensselaer Nanotechnology Center, Rensselaer Polytechnic Institute, 110 Eighth Street, Troy, New York 12180, United States

[‡]Materials Science and Engineering Department, Rensselaer Polytechnic Institute, 110 Eighth Street, Troy, New York 12180, United States

[§]Department of Electrical, Computer, and Systems Engineering, Rensselaer Polytechnic Institute, 110 Eighth Street, Troy, New York, 12180, United States

ABSTRACT: Nanoporous coatings have become the subject of intense investigation, in part because they have been shown to have unique and tailorable physical properties that can depart greatly from their dense or macroscopic counterparts. Nanoporous coatings are frequently fabricated utilizing oblique-angle or glancing-angle physical vapor-phase deposition techniques. However, a significant limitation for such coatings exists; they are almost always deposited on smooth and rigid planar substrates, such as silicon and glass. This limitation greatly constrains the applicability, tailorability, functionality and even the economic viability, of such nanoporous coatings. Here, we report our findings on nanoporous/polymer composite systems (NPCS) fabricated by utilizing oblique-angle electron-beam methodology. These unique composite systems exhibit several favorable characteristics, namely, (i) fine-tuned control over coating nanoporosity and thickness, (ii) excellent adhesion between the nanoporous coating and polymer substrate, (iii) the ability to withstand significant and repeated bending, and (iv) the ability to be molded conformably on two and three-dimensional surfaces while closely retaining the composite system's designed nanoporous film structure and, hence, properties.

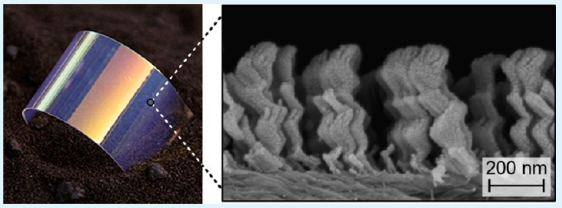

KEYWORDS: *nanoporous, thin-film, optical coating, conformable, polymer, oblique-angle*

1. INTRODUCTION

Nanoporous coatings[1,2] are particularly promising because of their physical property tailorability across a wide range of mechanical,[3,4] chemical,[5,6] optical,[7,8] electrical,[9,10] and structural[2] characteristics. That is, by controlling the specific nanostructure of a nanoporous film, the physical properties may be *arbitrarily* tailored within a broad range of desired values. Some examples of these unique and customizable physical properties include: surface area,[11] mass density and refractive index,[12] electrical[13] and thermal[14] conductivity, polarization,[15] hydrophobicity,[16] and magnetism.[17,18] By incorporation and maintenance of such tailorable properties with a flexible or moldable composite material system, new and far reaching functional pathways for nanoporous coatings emerge across a wide range of applications. Previously, only Co and Co−Ni coatings fabricated utilizing oblique-angle deposition on polymer substrates have been studied for their potential application to magnetic tape storage.[17,18] Yet, a much broader set of potential applications for conformable nanoporous/polymer composite systems (NPCS) exist, including optics (solar cells, light emitting diodes, displays, fiber optics, lenses and mirrors), gas and liquid sensors, production of scale (roll-to-roll processing), catalysts, and hydrogen storage.

For example, because of the availability of customizable and low-refractive index values, nanoporous coatings fabricated using oblique-angle deposition are reported to offer significant performance advantages for a variety of optical coating applications.[19,20] As such, we have designed and fabricated optical coatings consisting of single- and multilayer nanoporous coatings on a variety of polymer substrates with two main objectives. First, optical coatings utilizing NPCS represent a model system that demonstrates the compatibility and functionality of nanoporous coatings on polymers. Because an optical coating's performance is extremely sensitive to its physical properties, such as refractive index, thickness, features size, and absorption; a NPCS coating's optical characteristics can be used as a precise set of diagnostic tools in evaluating the capabilities and performance of this new composite system. Second, optical coatings utilizing nanoporous/polymer composites demonstrate one specific example of many important potential real-world applications.

2. RESULTS AND DISCUSSION

Employing the method of oblique-angle electron-beam deposition,[1,2] we fabricated SiO_2 and TiO_2 nanoporous coatings with a variety of porosities and thicknesses on a diversity of polymer substrates. Specifically, nanoporous coatings were successfully fabricated on polycarbonate, polyimide, polyester, polyolefin, and silicone sheets. In oblique-angle electron beam deposition methodology, the

Received: September 7, 2012
Accepted: November 1, 2012
Published: November 1, 2012

   dx.doi.org/10.1021/am301882m | ACS Appl. Mater. Interfaces 2012, 4, 6295−6301

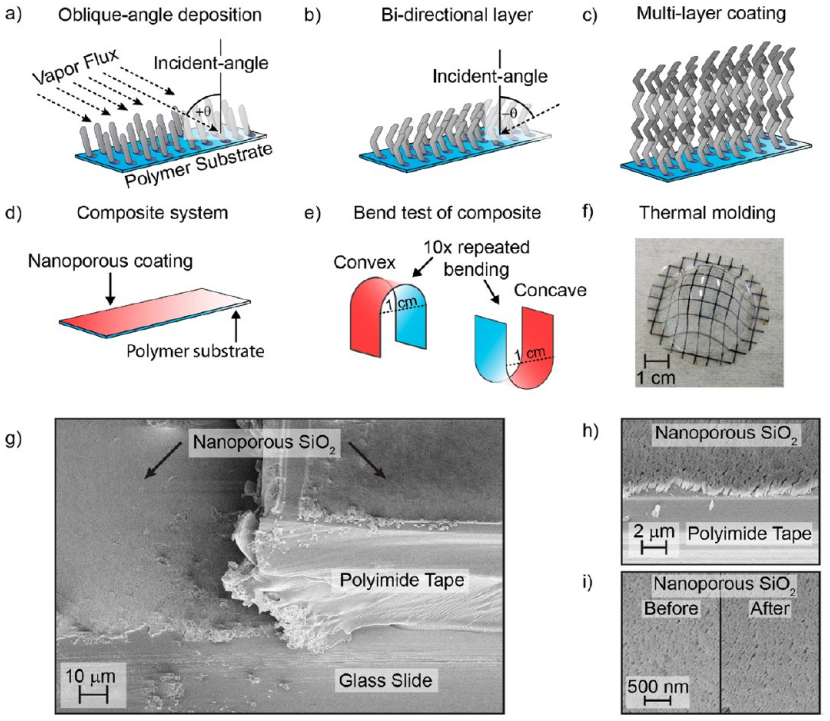

Figure 1. Schematic diagrams of (a) nanoporous film deposited by oblique-angle deposition with vapor flux of incident angle θ, (b) a bidirectional nanoporous film layer deposited with vapor flux incident angles $+\theta$ and $-\theta$, (c) multilayer nanoporous reflectance coating consisting of alternating layers of bidirectional SiO_2 and TiO_2, (d) a nanoporous coating first deposited on a flat polymer substrate, and (e) nanoporous coating and polymer substrate subjected to 10× repeated concave and convex bending around a 5 mm radius of curvature. (f) Photograph of a 5 mm square grid on a polycarbonate sheet thermally molded around a 1 in. diameter hemisphere. Scanning electron micrographs of (g) a 200 nm thick, 65% nanoporous SiO_2 film deposited on polyimide polymer tape with a glass backing substrate, (h) nanoporous SiO_2 film structure clearly visible on the surface of the polyimide tape, and (i) this nanoporous SiO_2 film surface on polyimide tape before and after bending.

polymer substrate is held at a fixed oblique-angle with respect to the deposition source and vapor flux, Figure 1a. Since nanoporous film growth is a self-organized process, no pretreatment of polymer substrates is necessary, and deposition conditions, such as temperature, deposition rate, and vapor pressure, are maintained at fixed conditions throughout. Additionally, to achieve a single nanoporous layer's overall thickness uniformity across large area samples, bidirectional layers of a desired nanoporosity are deposited using $+\theta$ incident angle for the first half of the layer thickness and $-\theta$ incident angle for the second half of the layer thickness, Figure 1b and c. The cross-sectional scanning electron micrograph (SEM) in Figure 1g illustrates one example of a NPCS coating: a 200 nm thick, 65% nanoporous SiO_2 film deposited on a polyimide tape substrate, which in turn is adhered to a glass slide. In this SEM image, the nanoporous coating is clearly visible on both the polyimide tape and glass substrates. Further magnified (Figure 1h and i), the nanostructure of the nanoporous SiO_2 film is readily apparent on the polymer substrate.

To investigate the physical-property tailorability of such coatings on polymer substrates, single-layer SiO_2 and TiO_2 nanoporous coatings were deposited on polycarbonate substrates across a range of fixed deposition angles (0−87°). Because of the extremely small feature size of such nanoporous coatings (much smaller than visible wavelengths of light), to a good approximation, such coating's effective refractive index can be considered to be a linear volume mixture of source material and air.[21] Using variable angle ellipsometry, we measured the effective refractive index values for SiO_2 and TiO_2 nanoporous coatings as a function of the deposition angle θ, plotted in Figure 2. As can be seen in the plots of Figure 2, both nanoporous SiO_2 and TiO_2 film porosity curves are smooth and well behaved, indicating that coatings of *any* porosity or refractive index may be fabricated on polymer substrates. This result suggests that other forms of nanostructured coatings will maintain their physical-property tailorability on polymer surfaces as well.

To examine the capabilities of NPCS coatings to withstand deformations such as bending and molding, optical coatings consisting of both single- and multilayer nanoporous coatings on transparent polymer substrates were designed[22] and fabricated. These conformable characteristics of the NPCS coatings are important both at the fabrication level (e.g., productions of scale such as roll-to-roll processing techniques) and at the application level, where such properties may be incorporated into the application itself (e.g., flexible displays). Optical coatings consisting of single-layer nanoporous coatings were fabricated on polymer substrates, Figure 1d, and were characterized using normal incidence optical reflectance and transmittance measurements. The NPCS optical coatings were then subjected to bending, repeated 10 times, with a radius of curvature of 5 mm, both in concave and convex directions, Figure 1e. Optical reflectance and transmittance measurements were then repeated. In Figure 3a and b, the measured transmittance of light (400−800 nm) for two NPCS coating examples is plotted for uncoated and coated transparent polyester sheets: (a) a 623 nm thick 70% nanoporous SiO_2 film and (b) a 212 nm 40% nanoporous SiO_2 film. No significant change in optical transmittance values was measured for either nanoporous coating as a result of repeated bending. These

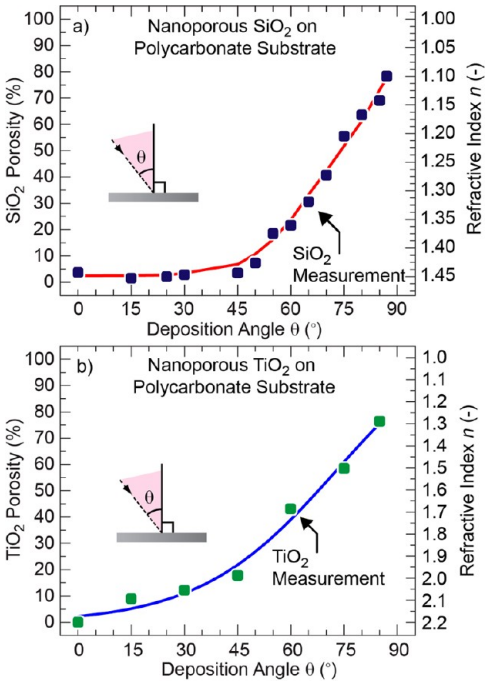

Figure 2. Refractive index and inferred nanoporosity plotted as a function of the deposition angle of nanoporous (a) SiO_2 and (b) TiO_2 coatings formed by electron-beam oblique-angle deposition. Included are hand drawn curves through the experimental data. Data points have less than 5% error.

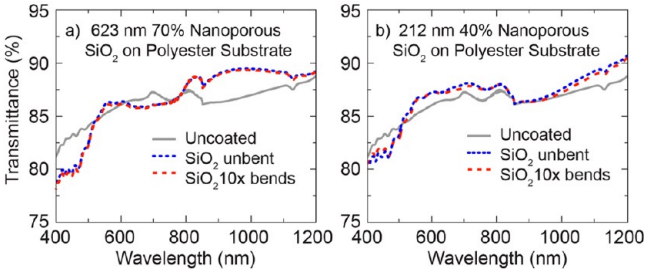

Figure 3. Measured transmittance values through (a) 623 nm, 70% nanoporous SiO_2, and (b) 212 nm, 40% nanoporous SiO_2 on polyester substrates before and after bending 10 consecutive times about a radius of curvature of 5 mm.

optical transmittance results were found to be quite general, and were chosen as representative optical behavior of NPCS coatings fabricated on polymer substrates over a range of porosity (10−90%) and thickness (50−800 nm) values. For these transmittance spectra, we note the presence of a discontinuity in the transmittance spectra at 850 nm, because of a change in diffraction gratings. Additionally, we note several features in the transmittance spectra near the wavelengths 650, 810, and 1120 nm. Because of the similarity of the transmittance spectra between the coated and uncoated polymer substrates, we attribute these features to be absorbance or scattering characteristics of this polymer film and not caused by the deposited nanoporous coatings.

In addition to single layer nanoporous NPCS coatings, multilayer reflection and antireflection (AR) coatings were designed, fabricated and optically characterized before and after the same bending conditions. Figure 4 plots the measured and calculated reflectance of: (a) a 4-layer reflectance coating consisting of alternating nanoporous layers, 129 nm thick 80%

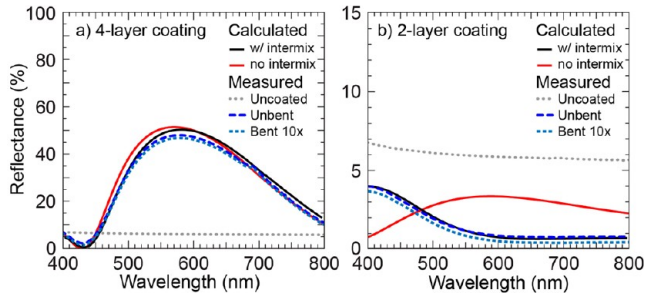

Figure 4. Measured reflectance values of (a) 4-layer nanoporous reflectance coating and (b) 2-layer nanoporous AR coating on polycarbonate substrates before and after bending about a radius of curvature of 5 mm, repeated 10 consecutive times. Calculated reflectance values with and without the presence of an interfacial layer between coating and substrate are also shown.

porous SiO_2 and 98 nm thick 65% porous TiO_2, on a transparent polycarbonate substrate and (b) a 2-layer antireflection (AR) coating consisting of SiO_2 layers, 52 nm thick 0% nanoporous and 240 nm thick 80% nanoporous, on a transparent polycarbonate substrate. As was found for single-layer NPCS coatings, multilayer NPCS coatings showed virtually no difference between measured reflectance values before and after the repeated bending. We have also computationally modeled the structures of the reflectance and AR optical coatings, shown in Figure 4, and calculated their corresponding reflectance values using the transfer-matrix method.[23] These reflectance values were found to be sensitive to the presence of an optically intermixed layer between polymer substrate and optical coating. NPCS coating models incorporating an interfacial layer (solid black line), are shown to have excellent agreement between modeled and measured results, while NPCS coating models not incorporating an intermixed layer between polymer substrate and optical coating (solid red line) did not show as good agreement. The discrepancy between calculated and measured reflectance values not incorporating an interfacial region is particularly apparent in the case of the 2-layer antireflection coating, Figure 4b.

It has been previously reported for dense coatings fabricated using plasma[24−26] and evaporation[27,28] based deposition methods, that a physically and optically intermixed layer, on the order of nanometers in thickness, forms between the polymer substrate and deposited coating.[29] In the case of electron-beam evaporations, such intermixed layers can reasonably be thought to occur because of the latent heat of the depositing condensate, the high energy ions, or X-ray radiation present during electron-beam evaporations.[30] As seen during the optical characterizations of our multilayer NPCS coatings, the presence of an intermixed layer of polycarbonate substrate, coating material, and fractional void (air), was necessary to account for the observed optical behavior. Accordingly, a 10−50 nm intermixed (half polymer/half 90% nanoporous material by volume) interfacial layer was incorporated into our ellipsometry-fitting and optical models. Such an intermixed layer was not only important to the modeling of our optical data, but it also helped to explain the observed excellent adhesion between our nanoporous films and polymer substrates.

As further evidence of the good adhesion and mechanical stability between the nanoporous film and polymer substrate, we present SEM images of the surface of a highly nanoporous SiO_2 film on a polyimide substrate (Figure 1i) and a cross-

section profile image of a 4-layer reflectance coating on polyimide tape (Figure 5), after bending as described above. In

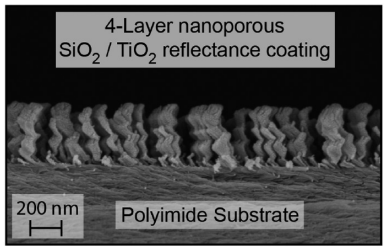

Figure 5. SEM image of optical reflectance coating consisting of four alternating layers of nanoporous SiO_2 and TiO_2 fabricated on a polyimide substrate. NPCS optical coating was subjected to bending about a radius of curvature of 5 mm, repeated 10 consecutive times.

both images, no visual evidence of change or damage to the micro- or nano-structure is seen, and these images are representative of the entire surface of the composite system. Importantly, these bending experiments demonstrate that such nanoporous coatings exhibit excellent adhesion characteristics to polymer substrates and further, are able to retain their structural and physical characteristics despite significant and repeated bending of the composite system.

Molding experiments were also performed on NPCS optical coatings. We categorize our molding experiments in three ways: In the first category, planar multilayer nanoporous coatings fabricated on polycarbonate substrates were heat formed around a cylinder with 5 mm radius of curvature. In this category of thermal molding, no significant change in surface area of the substrate or optical coating occurred. In the second category, the NPCS optical coatings were heat formed around a 1 in. diameter hemisphere, during which, stretching of the composite system resulted because of the projection that a two-dimensional surface onto a three-dimensional surface creates. Figure 1f shows an example of the resulting molded three-dimensional shape of the polycarbonate substrate with no optical coating. In the third category, the composite system was molded into an arbitrary free-form shape. The resulting molded NPCS optical reflectance coatings of each of these categories can be seen in the photographs in Figure 6.

Changes or damage of the nanoporous structure can manifest themselves as color changes, or more likely, as scattering or haziness of the transmitted and reflected light from the optical coatings. The optical coatings molded as in the first case, with no stretching (Figure 6a), exhibited no apparent change in optical quality and remain specular. Further, using a collimated light source (HeNe laser) and silicon photodetector, the optical transmittance of a 2-layer AR coating on polycarbonate film was measured before and after molding described in the first category. Despite such molding of the composite system, the optical transmittance was found to be identical in both measurements, 94 ± 1%, indicating that similar to the repeated bending tests, when the NPCS system is deformed so as to not change the coatings surface area, it is capable of such molding, while closely retaining the desired nanostructure and optical performance.

Inspecting the NPCS optical coatings heat molded as in the second category (Figure 6b), we used a 5 mm square grid drawn on the polycarbonate substrate, Figure 1f, to be able to measure the relative stretching of the NPCS optical coatings before and after molding. From these images, it is apparent that in areas of limited stretching, 0−15%, the coatings remain specular and maintain their original reflected color. Thus, the NPCS optical coating remains structurally stable and functionally intact at the relevant nanoscale in cases of limited stretching. However, in areas of significant stretching, 15−150%, significant haziness in the coating and substantial scattering of the reflected light is observed. Interestingly, visual inspection shows that this scattered light retains its reflected color. Therefore, we suggest that the more significant stretching of the NPCS coating results in microscopic defects that act as optical scattering sites. However, for the reflected color spectrum to be maintained, the essential underlying nanostructure of the NPCS coating must have survived the stretching process. Further evidence and discussion of this observation is presented below.

For NPCS optical coatings heat molded as in the third category, arbitrary convex and concave 3D curved surfaces were formed with the composite system. As can be seen in the photograph of Figure 6c, the NPCS optical coating retains its specular nature, and thus relevant nanostructure, even in areas of significant deformation. The third type of molding category

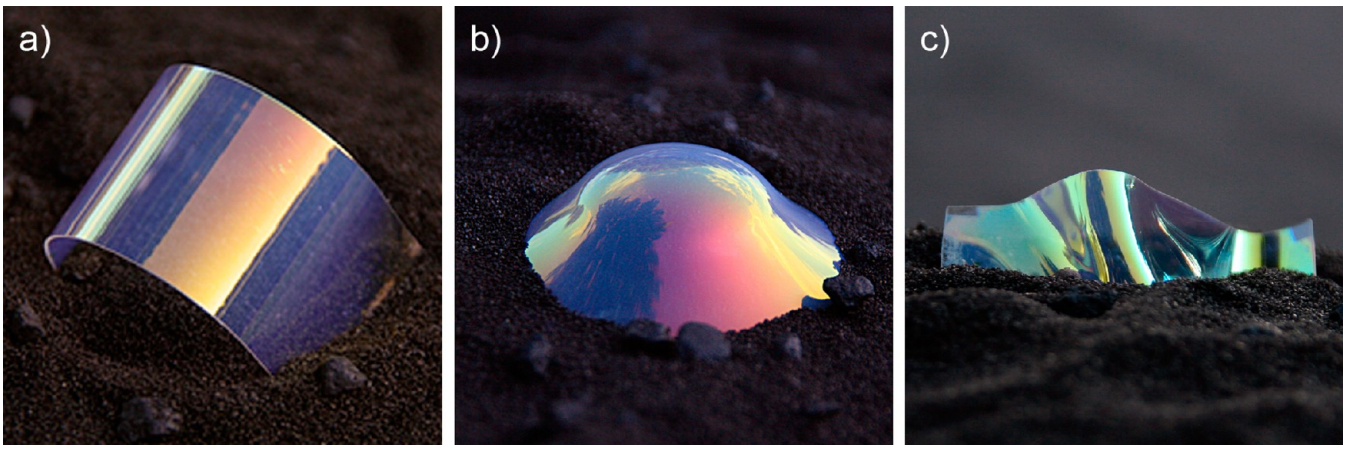

Figure 6. Photographic images of 4-layer optical reflectance coatings, of alternating layers of nanoporous SiO_2 and TiO_2, deposited on polycarbonate substrates and subsequently heat molded into three-dimensional shapes. (a) Blue reflectance coating heat molded around a 5 mm fixed radius. (b) Red reflectance coating heat molded around a 1 in. diameter hemisphere. (c) Free form heat molding of a blue/green reflectance coating.

demonstrates one potential pathway to fabricate such nanoporous coatings on complex surface topographies. As an example, NPCS coatings utilizing polyolefin films could be fabricated and subsequently shrink-wrapped on a wide variety of 3D surfaces, such as very high surface area shapes for catalytic or sensor technologies.

To begin to understand these observations, we examine the series of SEM images, Figure 7, of a 4-layer optical reflectance

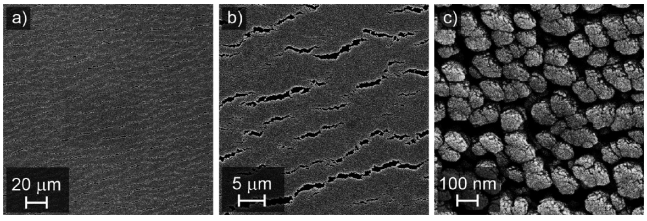

Figure 7. SEM surface image of an optical reflectance coating consisting of alternating layers of nanoporous SiO_2 and TiO_2 deposited on a polycarbonate substrate and subsequently heat molded into a 3D hemisphere. Progressively higher magnifications taken near the top of the molded hemisphere, an area of 0−15% stretching.

coating heat molded about a 1 in. hemisphere taken in an area of limited stretching, 0−15%. Inspection of Figure 7a shows that the NPCS coating is apparently uniform and well adhered to the polymer substrate. In Figure 7b, the formation of microfissures in the NPCS coating after 3D thermal molding can be seen. As expected, the relative size of the microfissures in the NPCS coating was found to correspond with the degree of stretch in the polymer substrate. Interestingly, however, despite the presence of microfissures, the density within the groupings of individual nanofeatures appears unchanged, Figure 7c. These results give strong evidence that, even in the case of significant stretching, the actual nanostructure of the coating itself receives minimal damage, is mechanically stable, and remains well adhered to the polymer substrate. Thus, while for specific applications (e.g., optical coatings), there may be practical limitations to the degree of NPCS stretching to retain a desired NPCS coating functionality, it seems likely that the existence of such microfractures would not be critical in the performance of a NPCS coating for many other applications, such as catalytic or sensor devices. It should also be noted that the presence and distribution of microfractures in a NPCS film will depend on the specific combinations of nanoporous material and polymer substrate chosen, as well as any additional polymer adhesion[29,31] treatments used.

Finally, for many potential applications and implementations of NPCS coatings, the ability of the coating to withstand abrasive loading forces will be of great importance.[32,33] As such, a simple abrasion test of highly nanoporous NPCS coatings was performed. Four single-layer, 200 nm thick 90% nanoporous SiO_2 coatings, were fabricated on polycarbonate sheets. Three of the NPCS coating surfaces were then loaded with 100, 250, and 500 g masses (approximately 1−5 N) onto a second 1 cm^2 uncoated polycarbonate sheet. This loaded polycarbonate sheet was then pulled horizontally, a single time, across the stationary NPCS coating surface. Subsequently, representative SEM images were taken for each of the three NPCS coating surfaces, along with images of the as-deposited NPCS surface, and are shown in Figure 8.

From this series of images, it can be seen that the 100 g cm^{-2} loaded NPCS coating surface (Figure. 8 b, f) did not sustain any observable damage to its nanostructure, and appears identical to the unloaded NPCS surface (Figure 8a, e). However, for the NPCS coating loaded with 250 g cm^{-2} visual inspection showed minor scratches on the coating surface. Further, the SEM images (Figure 8c, d) show small amounts of damage to the nanostructure, and also microscopic scratches interspersed over the surface of the coating. At the highest loading, 500 g cm^{-2} (Figure 8d, h), damage to the NPCS coating nanostructure is readily apparent, and microscopic scratches can be seen to span the length of the NPCS coating. These results confirm our laboratory observations that NPCS coatings, despite their high nanoporosity, are structurally robust and are able to withstand modest amounts of abrasion. These results are promising for NPCS coating applicability to productions of scale, such as roll-to-roll processing techniques.[34,35] However, for such applications involving abrasive loading forces, more detailed studies of the mechanical properties of such NPCS coatings are necessary.

The combined results of the bending, molding and abrasion experiments with NPCS coatings are highly encouraging and convincingly demonstrate their excellent adhesion and mechanical stability. Three main reasons are proposed for the apparent excellent adhesion and structural integrity of the NPCS coatings despite significant and/or successive deformations and minor abrasion. (i) Because of the extreme scale difference between that of the nanostructure (nm) and the bend radius (mm), no significant deformation takes place on the scale of the nanostructure itself. (ii) As described above, the presence of a physically intermixed layer of nanoporous material and polymer substrate ensures excellent adhesion.

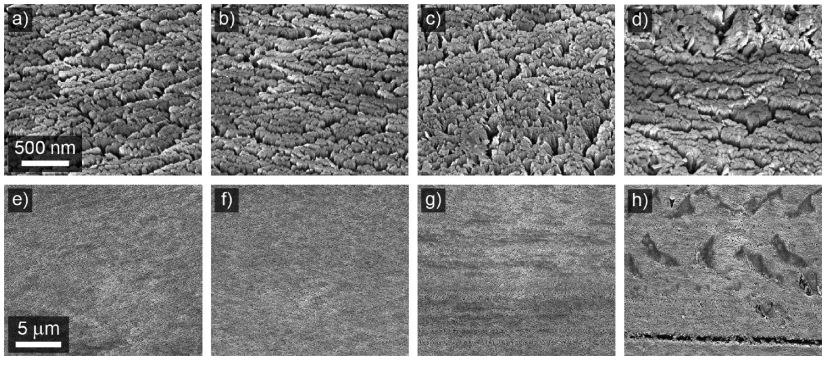

Figure 8. SEM surface images of 90% nanoporous SiO_2 deposited on a polycarbonate substrate (a, e) and subsequently abraded with (b, f) 100, (c, g) 250, and (d, g) 500 g cm^{-2}, loaded polycarbonate sheet.

(iii) It has previously been reported, that in addition to physical intermixing, chemical cross-linking occurs between dielectric coatings and polymer surfaces synthesized under high-energy deposition processing conditions.[29,32] Thus, not only is physical intermixing occurring, but potentially, chemical bonding takes place between the nanoporous coating and the polymer substrate because of the high energies present during electron-beam depositions. Physical intermixing and chemical bonding both provide important mechanisms for the observed excellent adhesion characteristics between these nanoporous coatings and their polymer substrates comprising our composite systems.

3. CONCLUSIONS

In summary, we have developed and presented a novel nanoporous/polymer composite system fabricated utilizing oblique-angle electron beam deposition methodology. Single and multilayer nanoporous coatings were deposited on polymer substrates and optically characterized. The presented composite system shares the rich tailorability and unique physical characteristic of such nanoporous coatings fabricated on rigid and planar substrates, yet differs significantly in its ability to be bent, molded, and stretched, while closely maintaining the important structural nanoscale characteristics despite substantial deformations of the polymer substrates. Further, these results are quite general and may be readily adopted for a wide variety of alternate material systems and compositions. This composite system provides a novel pathway to transition nanoporous coatings from a rigid and fixed 2D world to the freedom of a pliable 3D world. The end result is a potentially powerful new set of composite systems with wide applicability and greatly expanded functionality. The capabilities of nanoporous coatings newly introduced include flexibility, moldability, and stretchability, properties that are important either at the fabrication and implementation level or as qualities desired in a final product. Among the applications that can directly benefit from such composite systems, are optic, electronic, sensing, and catalytic devices in areas, such as flexible displays, flexible solar cells, and hydrogen-fuel storage systems, as well as potentially enabling productions of scale such as roll-to-roll processing techniques.

4. EXPERIMENTAL SECTION

SiO_2 and TiO_2 nanoporous coatings were deposited on polymer substrates utilizing oblique-angle electron-beam deposition. Growth conditions were held constant throughout. Pressure during SiO_2 depositions was at or below 1.5×10^{-6} Torr with no reactive gases. TiO_2 coatings were deposited in the presence of O_2 maintained at a pressure of 1.5×10^{-4} Torr. Deposition rate was maintained at 0.2 nm s^{-1} and monitored with a quartz crystal sensor for both SiO_2 and TiO_2 coatings. The polymer substrates were held in place by a motorized variable-angle mount, with a source-to-substrate throw distance of approximately 20 cm. Deposition angle, $+\theta$ and $-\theta$, was held fixed but alternated for the half-thickness of each layer. No pretreatment of the polymer substrates was used, and deposition occurred at approximately room temperature. Spectroscopy and ellipsometry measurements were performed using the following: a normal incidence JASCO UV−vis/NIR spectrometer and a J.A. Woollam variable angle ellipsometer (60°, 65°, and 70°). By assuming a linear volume approximation and using both an effective medium approximation (EMA) and Cauchy fitting models, we determined the refractive index, porosity and thickness of the single-layer SiO_2 and TiO_2 nanoporous coatings. No appreciable difference was found between the EMA and Cauchy fitting models. Molding of the polycarbonate substrates was done with a custom-built, gravity force fed positive-shaped heat mold in a standard laboratory oven heated to 165 °C. Scanning electron microscopy was done using a Carl Zeiss Supra SEM. The stretching of the NPCS was characterized using a 5 mm square grid on a transparent polycarbonate film, measured before and after molding and stretching.

AUTHOR INFORMATION

Corresponding Author

*E-mail: poxsod2@rpi.edu. Address: 110 Eighth Street, Nanotechnology Center, MRC Troy NY, 12180.

Author Contributions

The manuscript was written through contributions of all authors. All authors have given approval to the final version of the manuscript.

Funding

This material is based upon work supported by the National Science Foundation under grant number DMR-0642573, DOE support under grant number DE-FG02-06ER46347, and by NYSTAR under contact number C070119. The authors also gratefully acknowledge support by Samsung LED, Sandia National Laboratories, Magnolia Solar Inc., Crystal IS, and Troy Research Corporation.

Notes

The authors declare no competing financial interest.

ABBREVIATIONS

SEM, scanning electron micrograph; NPCS, nanoporous/polymer composite system; AR, antireflection; EMA, effective medium approximation

REFERENCES

(1) Hawkeye, M. M.; Brett, M. J. *J. Vac. Sci. Technol., A* **2007**, *25*, 1317−1335.
(2) Steele, J. J.; Brett, M. J. *J. Mater. Sci: Mater. Electron.* **2006**, *18*, 367−379.
(3) Seto, M. W.; Robbie, K.; Vick, D.; Brett, M. J.; Kuhn, L. *J. Vac. Sci. Technol., B: Microelectron. Nanometer Struct.* **1999**, *17*, 2172−2177.
(4) Zhang, G. *J. Appl. Phys.* **2004**, *95*, 267−271.
(5) Tai, W.-P.; Oh, J.-H. *Sens. Actuators, B* **2002**, *85*, 154−157.
(6) Sanchez, C.; Boissière, C.; Grosso, D.; Laberty, C.; Nicole, L. *Chem. Mater.* **2008**, *20*, 682−737.
(7) Xi, J.-Q.; Kim, J. K.; Schubert, E. F. *Nano Lett.* **2005**, *5*, 1385−1387.
(8) Xi, J.-Q.; Schubert, M. F.; Kim, J. K.; Schubert, E. F.; Chen, M.; Lin, S. Y.; Liu, W.; Smart, J. A. *Nat. Photonics* **2007**, *1*, 176−179.
(9) Park, S.-J.; Kim, K. S.; Eden, J. G. *Appl. Phys. Lett.* **2005**, *86*, 221501.
(10) Demoustier-Champagne, S.; Stavaux, P.-Y. *Chem. Mater.* **1999**, *11*, 829−834.
(11) Krause, K. M.; Taschuk, M. T.; Harris, K. D.; Rider, D. A.; Wakefield, N. G.; Sit, J. C.; Buriak, J. M.; Thommes, M.; Brett, M. J. *Langmuir* **2010**, *26*, 4368−4376.
(12) Poxson, D. J.; Mont, F. W.; Schubert, M. F.; Kim, J. K.; Schubert, E. F. *Appl. Phys. Lett.* **2008**, *93*, 101914.
(13) Heo, Y. W.; Tien, L. C.; Norton, D. P.; Kang, B. S.; Ren, F.; Gila, B. P.; Pearton, S. J. *Appl. Phys. Lett.* **2004**, *85*, 2002−2004.
(14) Abramson, A. R.; Kim, W. C.; Huxtable, S. T.; Yan, H.; Wu, Y.; Majumdar, A.; Tien, C. L.; Yang, P. *J. Microelectromech. Syst.* **2004**, *13*, 505−513.
(15) Wu, Q.; Hodgkinson, I. J.; Lakhtakia, A. *Opt. Eng.* **2000**, *39*, 1863−1868.
(16) Zhang, L.; Singh, S.; Tian, C.; Shen, Y. R.; Wu, Y.; Shannon, M. A.; Brinker, C. J. *J. Chem. Phys.* **2009**, *130*, 154702.
(17) Lisfi, A.; Lodder, J. C. *J. Magn. Magn. Mater.* **2002**, *242*, 370−373.

(18) Lisfi, A.; Lodder; Wormeester, H.; Poelsema, B. *Phys. Rev. B: Condens. Matter Mater. Phys.* **2002**, *66*, 174420.
(19) Poxson, D. J.; Schubert, M. F.; Mont, F. W.; Schubert, E. F.; Kim, J. K. *Opt. Lett.* **2009**, *34*, 728−730.
(20) Poxson, D. J.; Mont, F. W.; Schubert, M. F.; Kim, J. K.; Cho, J.; Schubert, E. F. *Opt. Express* **2010**, *18*, 594−599.
(21) Southwell, W. H. *Appl. Opt.* **1985**, *24*, 457−460.
(22) Schubert, M. F.; Mont, F. W.; Chhajed, S.; Poxson, D. J.; Kim, J. K.; Schubert, E. F. *Opt. Express* **2008**, *16*, 5290−5298.
(23) Born, M.; Wolf, E. In *Principles of Optics*; Pergamon Press: Oxford, U.K., 1980; p 51−70.
(24) Poitras, D.; Martinu, L. *Appl. Opt.* **2000**, *39*, 1168−1173.
(25) Bergeron, A.; Poitras, D.; Martinu, L. *Opt. Eng.* **2000**, *39*, 825−831.
(26) Martinu, L.; Poitras, D. *J. Vac. Sci. Technol., A* **2000**, *18*, 2619−2645.
(27) Dennler, G.; Houdayer, A.; Raynaud, P. *Plasmas Polym.* **2003**, *8*, 43−59.
(28) Da Silva Sobrinho, A. S.; Schühler, N.; Klemberg-Sapieha, J. E.; Wertheimer, M. R.; Andrews, M.; Gujrathi, S. C. *J. Vac. Sci. Technol., A* **1998**, *16*, 2021−2030.
(29) Leterrier, Y. *Prog. Mater. Sci.* **2003**, *48*, 1−55.
(30) Ohring, M. In *The Materials Science of Thin Films*, 2nd ed.; Academic Press: San Diego, CA, 1992; p 121−126.
(31) Awaja, F.; Gilbert, M.; Kelly, G.; Fox, B.; Pigram, P. J. *Prog. Polym. Sci.* **2009**, *34*, 948−968.
(32) Bergeron, A. *J. Vac. Sci. Technol., A* **1998**, *16*, 3227−3234.
(33) Rats, D.; Martinu, L.; Stebut, J. *Surf. Coat. Technol.* **2000**, *123*, 36−43.
(34) Sierros, K. A.; Morris, N. J.; Kukureka, S. N.; Cairns, D. R. *Wear* **2008**, *267*, 625−631.
(35) Sondergaard, R.; Hosel, M.; Angmo, D.; Larsen-Olsen, T. T.; Krebs, C. *Mater. Today* **2012**, *15*, 36−49.